

# Risperidone Powder Prepared by Spray Drying Technology for Intranasal Delivery

Ting Li<sup>1,a</sup>, Jingyu Shi<sup>1,b</sup>, Zhengbo Tong<sup>1,\*</sup>, Hao Miao<sup>2</sup>

<sup>1</sup>Center for Simulation and Modeling of Particulate Systems, Southeast University-Monash University Joint Research Institute, Suzhou, Jiangsu, PR China

<sup>2</sup>Department of Chemical Engineering Monash University Clayton, Vic, Australia

**Abstract:** The main objective of this study was to prepare Risperidone (RIS) nasal powder by spray drying method, so as to achieve controlled drug release and high deposition efficiency in the nasal cavity. The microparticles with uniform size and controllable structure were prepared by mixing hydroxypropyl- $\beta$ -cyclodextrin (CD) with API before a novel microfluidic spray drying technology. The properties of particles were characterized in terms of particle size, crystal shape and in vitro local deposition efficiency, and the formation mechanism and structure-activity relationship of particles were revealed. The results showed that the spray drying samples were all in amorphous state, and the physicochemical properties of risperidone can be improved by the addition of CD. Compared to spray-dried pure RIS, spray-dried samples with CD addition had good fluidity (CI<30%) and more suitable particle sizes (35-55 $\mu$ m) for nasal delivery. When the mass ratio of drug excipients (RIS: CD) was 1:6, the deposition fraction in the olfactory region was 13.338%, indicating that this prescription has considerable potential for brain targeted delivery.

## 1 INTRODUCTION

Schizophrenia is a serious mental illness with high relapse rate and high disability rate. Risperidone, as a second-generation antipsychotic, has the advantages of low extrapyramidal side effects and good tolerance. At present, risperidone dosage forms used in clinical treatment mainly include oral tablets, solution and long-acting slow-release microspheres for injection. However, Risperidone oral preparation has first-pass effect, injection is expensive and has safety problems.

In recent years, nasal administration, as a non-invasive alternative, has been shown to bypass the blood-brain barrier and directly enter the central nervous system via the olfactory area and trigeminal pathway. Compared with other administration methods, nasal administration not only avoids drug loss caused by first-pass metabolism, but also minimizes systemic drug exposure, effectively avoiding the risk of side effects (Privalova, 2012). In order to improve the efficiency of drug brain-targeted delivery, intranasal administration needs to deal with the problem of limited drug residence time due to nasal ciliary clearance. For this problem, solid formulations have significant advantages over liquid formulations. Nasal powder has simple ingredients, better physicochemical and microbial stability, and allows higher dosage. By adding excipients, a longer nasal mucosa residence time can be obtained, which can promote the diffusion and absorption of drugs in

the mucosa, thereby improving the bioavailability of drugs (Bale, 2016).

The purpose of this study is to prepare a risperidone nasal powder with simple composition, stable structure and high deposition rate in the olfactory area by spray drying technology. In this study, a self-built microfluidic spray drying tower (MFSD) was used to produce particles with uniform particle size and controllable structure. Hydroxy- $\beta$ -cyclodextrin has been proved to be an absorption enhancer for nasal administration, and solubilization can be achieved through inclusion of active molecules, so cyclodextrin was selected as an excipient for the insoluble drug risperidone in this study. The physical and chemical properties of the spray-dried particles were characterized by SEM, XRD and FTIR. Evaluation of nasal delivery and deposition performance of spray-dried particles using a 3D-printed real human nasal cavity model.

## 2 MATERIALS AND METHODS

### 2.1 Chemicals and Reagents

Risperdal (RIS, MW 410.49g/mol) was purchased from Shanghai Macklin Biochemical Co., Ltd. (Shanghai, China). Hydroxypropyl- $\beta$ -cyclodextrin (CD; purity >99%, MW 1541.54 g/mol) was obtained from Shanghai Titan Technology Co., Ltd. (Shanghai, China). Deionized water (~18.2 M $\Omega$ /cm) was purified using a Milli-Q water system

<sup>a</sup> email: 1106810853@qq.com

<sup>b</sup> email: 2116451422@qq.com

\* Corresponding author: e-mail: z.tong@seu.edu.cn

(Merck, Darmstadt, Germany) throughout the experiments. All other chemicals and solvents were of analytical grade.

## 2.2 Fabrication of RIS Spray-Dried Microparticles

The composition of the liquid feed is summarized in Table 1. RIS and CD were weighed according to the drug-to-

polymer ratio (D/P) of 1:9, 1:6 and 1:3 respectively, and the mass ratio of ethanol to deionized water in all prepared solution mixtures was 1:1. The liquid was filtered by a 0.45µm filter membrane to obtain spray drying feed solution. The feed solution was atomized into small droplets by the nozzle into the drying chamber. During the spray drying, a water bath was employed to keep the temperature of the feed solution at 35°C.

**Table 1** Precursor formulation and process parameters for spray drying.

Formulation ID	Liquid Feed composition			Drying temperature (°C)	
	RIS (g/100g solution)	HPBCD (g/100g solution)	Ethanol (g): Water(g)	Inlet	Outlet
SD-RIS-1.0	1	/	1: 1	140	40-50
SD-R1CD3-1.0	0.25	0.75	1: 1	180	50-60
SD-R1CD3-1.5	0.375	1.125	1: 1	180	50-60
SD-R1CD6-1.0	0.143	0.857	1: 1	180	50-60
SD-R1CD6-1.5	0.214	1.286	1: 1	180	50-60
SD-R1CD9-1.0	0.1	0.9	1: 1	180	50-60
SD-R1CD9-1.5	0.15	1.35	1: 1	180	50-60

## 2.3 Particle Characterization Studies

### 2.3.1 Flow properties:

The bulk density ( $\rho_b$ ) was determined by loosely filling a weighed amount of powder into a 5 mL measuring cylinder; the tapped density ( $\rho_t$ ) was the ultimate (equilibrium) density after the graduated cylinder tapped no less than 100 times until the volume of the particles inside remained unchanged.

The microparticles flowability was characterized by Carr's index (CI) calculated by Eq. (1):

$$CI = \frac{\rho_t - \rho_b}{\rho_t} \cdot 100\% \quad (1)$$

CI > 25% indicates poor flowability (Carr, 1965). The average density of each sample was based on three repeat experiments.

### 2.3.2 Particle Size and Morphology analysis:

Scanning electron microscope (SEM, S-4700, Hitachi High Technologies Corporation, Japan) was used to characterize the powder morphology. Sputter-coated with platinum at a current of 50 mA after sample powder was placed to the sample preparation table with conducting carbon tape. The

electrical conductivity of the particles was improved and avoid charge build-up during observation in the SEM.

The images were processed with Image J software and the average particle size was obtained according to Eq. (2):

$$\bar{d} = \sum_{i=1}^n \frac{d_i}{N} \quad (2)$$

### 2.3.3 X-ray diffraction analysis (XRD):

Powder X-ray diffraction (XRD) patterns of RIS raw material and spray-dried microparticles was obtained by a desktop diffractometer (D2 PHASER, Bruck, Germany) Radiation was derived from a Cu-K $\alpha$  ( $\lambda = 1.54056 \text{ \AA}$ ) source at 30 kV and a current of 10 mA. The scanning angle ranged from 10° to 60° (2 $\theta$  basis) with a step size of 0.02° and 0.2 s for each step.

### 2.3.4 Fourier transformed infrared Spectroscopy analysis (FT-IR):

Fourier transform infrared (FT-IR) spectra analyses were performed with a Bruker tensor 27 spectrometers (Bruker, Germany) with a resolution of 4cm<sup>-1</sup> and a wavenumber range of 400 cm<sup>-1</sup> to 4000 cm<sup>-1</sup>.

### 2.3.5 *In vitro* nasal deposition performance:

Aerodynamic assessment of the dry powder formulations for nasal administration was performed in a nasal cast model. The nasal cavity model was developed based on computed tomography (CT) scan of a 59-year-old Asian female adult's nose.

The nasal cavity model is divided into five sections, representing nasal vestibule, lower turbinate, middle turbinate, olfactory area, and nasopharynx region (Fig. 1.a) to quantitate the deposition pattern within the nasal cavity. The inner surface of the nasal casts was coated with 1% (v/v) Tween 20 in methanol and allowed to dry to minimize deviations caused by particle bounce (Thakkar, 2018).

During the nasal delivery experiments, the dry powder formulation (20 mg) was applied to the nasal cast using a simplified 3D-printed dry powder delivery device (Fig. 1.b). Accurately weigh the delivery device before and after the experiment to determine the actual amount of sample delivered.

The angle of administration was fixed at 60° from horizontal, and the tip of the device was inserted into the nasal vestibule at a depth of 5mm. Air flow was provided by a breathing simulator, which was set to exhale in a sinusoidal pattern with a peak value of 50 L/min.

After administration, each part of the nasal cast was carefully washed with 50 mL deionized water. The concentration of risperidone from the wash was analyzed by UV absorbance at a wavelength of 276 nm. The percentage of risperidone deposited in each region was calculated from the amount measured in the four parts divided by the total amount of risperidone measured.

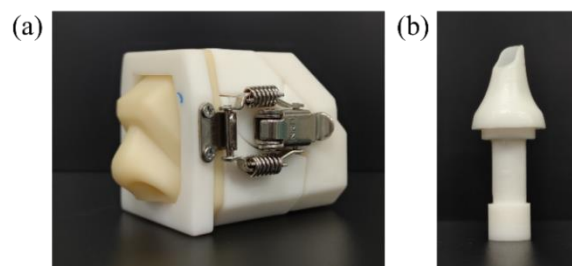


**Figure 1.** The 3D-printed nasal cast (a); 3D-printed nasal powder delivery device (b).

## 3 RESULTS AND DISCUSSION

### 3.1 Particle Size, Morphology and Density

Uniform CD-RIS microparticles were successfully prepared by spray drying technique with the feed solution formulation shown in the table 2. Table 2 summarizes the physical properties of the spray dried samples, including particle geometry size, density and Carr's Index (CI). The spray-dried samples had particle sizes between 35 and 55µm and a narrow particle size distribution, which met the standard for nasal inhalation powder. The particle size of SD-RIS was larger than that of the CD-RIS co-spray, mainly because the solubility of RIS is much lower than that of CD, leading to the precipitation of the RIS molecules in a shorter period of time, which accelerated the formation of the shell layer and resulted in larger spray-dried particles.

**Table 2** Summary of the physical properties of the different formulations

Sample	Particle size (µm)	Bulk density (g/cm <sup>3</sup> )	Tapped density (g/cm <sup>3</sup> )	CI (%)
SD-RIS-1.0	86.54±7.71	/	/	/
SD-R1CD3-1.0	35.71±3.18	0.661±0.02	0.842±0.01	21.57±2.91
SD-R1CD3-1.5	39.58±3.24	0.684±0.02	0.859±0.01	20.39±1.10
SD-R1CD6-1.0	36.67±4.47	0.579±0.02	0.757±0.02	23.53±1.86
SD-R1CD6-1.5	46.17±4.43	0.534±0.01	0.705±0.02	24.37±2.52
SD-R1CD9-1.0	44.54±5.33	0.378±0.01	0.545±0.02	30.68±2.10
SD-R1CD9-1.5	51.13±4.63	0.372±0.01	0.535±0.01	30.46±2.21

The SEM images of spray drying samples was shown in Figure 2. The SD particles showed different morphological characteristics depending on the ratio of CD to RIS, with the particles prepared in the ratio of 1:3 being solid spherical with smooth surface. The ratio of 1:6 is closer to spindle shape, while the ratio of 1:9 shows a wrinkled spherical shape. The variation in morphology is mainly influenced by the percentage of CD in the feed solution. When the proportion of CD in the feed solution

increased, the geometric diameter of the particles prepared by spray drying with the same solid content was larger. This was because the diffusion rate of RIS in the droplet was inconsistent with that of CD, resulting in the non-synchronous shrinkage of the surface and the formation of a folded surface.

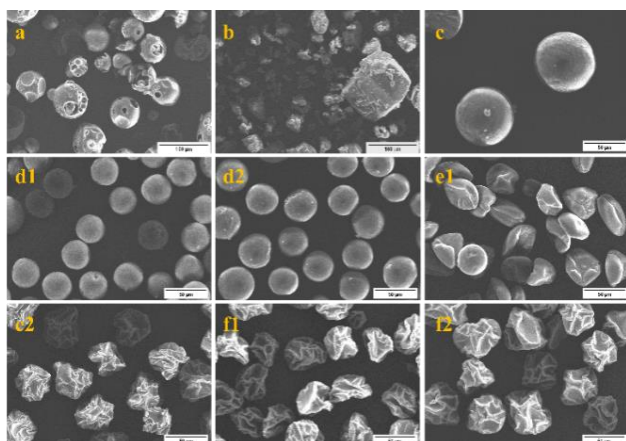


**Figure 2.** SEM images of raw HCD (a), raw RIS (b), and SD-RIS-1.0wt% (c); SD-RICD3-1.0wt% (d1), SD-RICD3-1.5wt% (d2), and SD-RICD6-1.0wt% (e1); SD-RICD6-1.5wt% (e2), SD-RICD9-1.0wt% (f1), SD-RICD9-1.5wt% (f2).

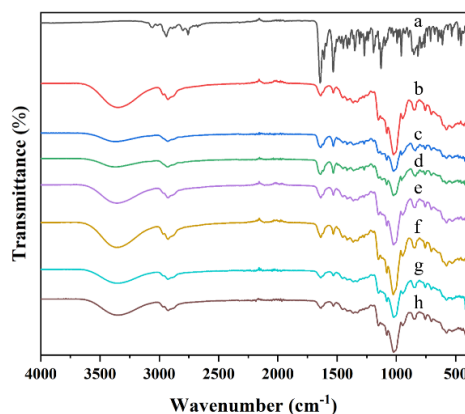


**Figure 4.** FT-IR spectra of raw RIS (a), raw HPMC (b), SD-RICD3-1.0wt% (c), SD-RICD3-1.5wt% (d), SD-RICD6-1.0wt% (e), SD-RICD6-1.5wt% (f), SD-RICD9-1.0wt% (g), SD-RICD9-1.5wt% (h), respectively.

### 3.2 Particle Crystal Property and Storage Stability

From the XRD patterns (Figure 3), it can be seen that the pure RIS has a more obvious signal peak, indicating that it presents a crystalline structure in its natural state. The XRD results of spray-dried microparticles all show a broader amorphous carbon inclusion peak near  $20^\circ$ , indicating that RIS undergoes inclusion interaction with CD to form an amorphous structure, which also indicates that RIS is well dispersed in the CD matrix. The FT-IR spectral scan results (Figure 4) also confirmed the occurrence of inclusion interaction. The FT-IR spectra of the spray-dried sample powder showed that the signal of the vibrational peaks was significantly weakened, indicating that the RIS molecules were embedded in the CD cavity structure and thus some of the vibrational peaks were masked.

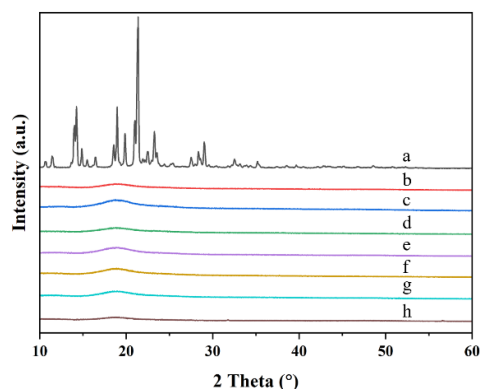


**Figure 3.** XRD patterns of raw RIS (a), raw HPMC (b), SD-RICD3-1.0wt% (c), SD-RICD3-1.5wt% (d), SD-RICD6-1.0wt% (e), SD-RICD6-1.5wt% (f), SD-RICD9-1.0wt% (g), SD-RICD9-1.5wt% (h), respectively.

### 3.3 In Vitro Nasal Deposition Performance

The spray drying sample powder with 1% solid content in the feed solution was selected to investigate the regional deposition performance of nasal model. As can be seen from Figure 5, at a simulated respiratory flow rate of 50 L/min, spray dried sample powder with CD added was effectively released, showing that more than 90% of the dose was delivered to the nasal cavity, while in contrast, only 31.27% of the dose of pure RIS spray dried powder was delivered to the nasal cavity. On the one hand, the reason may be that the fluidity of pure RIS spray dry powder is poor, the powder is easy to caking, resulting in the delivery dose decrease. On the other hand, the addition of cyclodextrin effectively improved the sphericity and fluidity of the particles. In addition, all spray-dried samples with CD showed good deposition rates in the olfactory region, which were  $10.20 \pm 0.17\%$ ,  $13.34 \pm 0.73\%$  and  $9.96 \pm 0.41\%$ , respectively.

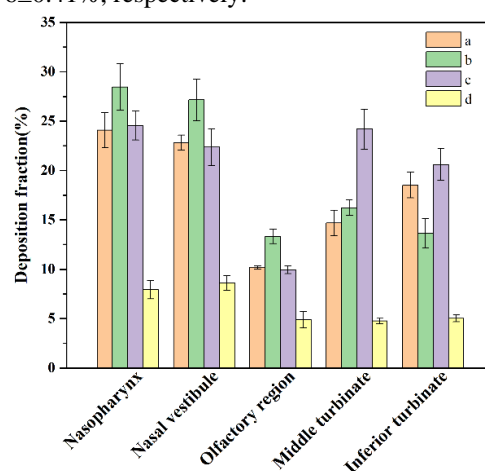


**Figure 5.** Regional deposition fractions of different formulations: SD-RICD3-1.0wt% (a), SD-RICD6-1.0wt% (b), SD-RICD9-1.0wt% (c), SD-RIS-1.0wt% (d).

## 4 CONCLUSION

In this study, using risperidone as a model drug, a series of risperidone powders suitable for nasal administration were successfully prepared by spray drying technology. The particle structure of the powder was characterized and the delivery characteristics of the nasal powder aerosol were evaluated on an in vitro nasal cavity 3D printed model. The spray-dried sample particles with the adding of cyclodextrin was amorphous, with uniform particle size between 35-55 microns, which was suitable for nasal administration. The results of the nasal cavity model showed that SD-R1CD6-1% sample had the highest olfactory area deposition fraction (13.338%), which was 2.73 times that of SD-RIS-1% olfactory area deposition rate (4.884%), showing that the spray-dried sample had the highest Potential of intranasal drug delivery for the treatment of brain disorders.

## ACKNOWLEDGMENT

The authors are grateful to the National Key R&D Project of China (2021YFB1715500) for the financial support of this work.

## REFERENCES

1. Bale, S.; Khurana, A.; Reddy, A.S.S.; Singh, M.; Godugu, C. Overview on therapeutic applications of microparticulate drug delivery systems. *Crit. Rev. Ther. Drug Carr. Syst.* 2016, 33, 309–361.
2. Carr, R.L. Evaluating flow properties of solids. *Chem. Eng. J.* 1965, 18, 163–168.
3. Privalova, A.M.; Gulyaeva, N.V.; Bukreeva, T.V. Intranasal administration: A prospective drug delivery route to the brain. *Neurochem. J.* 2012, 6, 77–88.
4. Thakkar, S.G.; Warnken, Z.N.; Alzhrani, R.F.; Valdes, S.A.; Aldayel, A.M.; Xu, H.; Williams, R.O., III; Cui, Z. Intranasal immunization with aluminum salt-adjuvanted dry powder vaccine. *J. Control. Release* 2018, 292, 111–118.